Liquid Crystals
Publication details, including instructions for authors and subscription information:
http://www.informaworld.com/smpp/title~content=t713926090

Polycatenar mesogens with a perfluorinated moiety showing a variety of liquid crystalline polymorphism

Etsushi Nishikawa[a]; Jun Yamamoto[a]; Hiroshi Yokoyama[a]
[a] Yokoyama Nano-structured Liquid Crystal Project, ERATO, Japan Science and Technology Agency, TRC 5-9-9 Tokodai, Tsukuba, Ibaraki 300-2635, Japan

To cite this Article Nishikawa, Etsushi , Yamamoto, Jun and Yokoyama, Hiroshi(2005) 'Polycatenar mesogens with a perfluorinated moiety showing a variety of liquid crystalline polymorphism', Liquid Crystals, 32: 5, 585 — 598
To link to this Article: DOI: 10.1080/02678290500115880
URL: http://dx.doi.org/10.1080/02678290500115880

Liquid Crystals, Vol. 32, No. 5, May 2005, 585–598

Taylor & Francis
Taylor & Francis Group

Polycatenar mesogens with a perfluorinated moiety showing a variety of liquid crystalline polymorphism

ETSUSHI NISHIKAWA*, JUN YAMAMOTO and HIROSHI YOKOYAMA

Yokoyama Nano-structured Liquid Crystal Project, ERATO, Japan Science and Technology Agency, TRC 5-9-9 Tokodai, Tsukuba, Ibaraki 300-2635, Japan

(*Received 30 August 2004; in final form 20 December 2004; accepted 30 December 2004*)

Polycatenar materials composed of a four-aromatic-ring core, with either a bulky or end-branched perfluorinated moiety attached at one end through a methylene spacer group, and three peripheral alkoxy chains of varying length (the carbon number n=4, 6, 8, 10, 12, 14, 16) on the other end-ring, were synthesized to investigate the roles of the chemical structure of the compositional segments in relation to liquid crystalline phase formation. It was found that a homologous series of polycatenar materials exhibited a variety of liquid crystalline phases strongly dependent on the length of the peripheral alkyl chains. Moreover it was shown that changes in the spacer group and in the structure of the perfluorinated segment had a significant influence on mesophase formation.

1. Introduction

During the last two decades, since the development of discotic mesogens by Chandrasekhar *et al.* and Billard *et al.* [1, 2], new mesogenic materials with a variety of unique, non-conventional molecular shapes have been investigated. Liquid crystalline (LC) phases with intriguing microstructure have been found, which has considerably improved the understanding of structure–property relationships in the LC field [3–5]. Among these new materials polycatenar compounds are fascinating mesogenic materials, first reported in 1985 by Malthête *et al.*[6] These materials were designed as a combined structure of rod-like and disc-like mesogens, generally consisting of a long aromatic core and several peripheral alkyl chains [7]. Owing to the unusual molecular shape and the chemical difference between hard-core segments and flexible peripheral chains, a variety of mesophases (e.g. nematic, smectic, columnar and cubic) have been observed in this class of materials, the number, position and length of the peripheral alkyl chains playing a crucial role in the organization into LC phases [8–10]. Moreover the influence of the structural segments (e.g. the length of the core, the shape of linking groups and substituents, etc.) on the formation of mesophases has been recognized [7, 11–13]. The studies on polycatenar materials have also been expanded to metallomesogenic systems [14–19].

Perfluorinated substituents have been incorporated into rod-like and disc-like mesogens; they can enhance the segregation power owing to their high incompatibility with hydrocarbon moieties [20–23]. Thus, materials with perfluorinated chains tend to form LC phases with a micro-segregated structure [24–27]. The first polycatenar materials with a perfluorinated substituent were reported in 1991 [28, 29]. One was a four-ring cored tetracatenar mesogen with a perfluorooctyloxy chain, which was found to form only one (cubic) LC phase [28]. Another system involved three-ring cored tricatenar materials, which exhibited smectic mesomorphism [29]. Since then several polycatenar mesogens having a perfluorinated moiety have been synthesized [12]; however their phase behaviour has not been systematically investigated.

We have recently begun to investigate new polycatenar materials with a perfluorinated moiety [30, 31]. In the present work, firstly, the LC phase behaviour of a homologous series of new tetracatenar mesogens is reported. These are composed of a four-aromatic-ring core with a bulky perfluorinated moiety attached to one terminal ring through an alkyl chain spacer, and three peripheral alkoxy chains of varying length n (n=the number of carbon atoms in the alkyl chain) on the other end-ring. We show that this homologous series of polycatenar materials exhibits rich mesomorphism strongly dependent on the length of peripheral alkyl chains. Secondly, with the peripheral alkyl chain length

*Corresponding author. Email: etsushi.nishikawa@ihara-chem.co.jp; present address: Advanced Materials Department, Ihara Chemical Industry Co., Ltd, 2256 Nakanogo, Fujikawa-cho, Ihara-gun, Shizuoka 421-3306, Japan.

Liquid Crystals
ISSN 0267-8292 print/ISSN 1366-5855 online © 2005 Taylor & Francis Group Ltd
http://www.tandf.co.uk/journals
DOI: 10.1080/02678290500115880

fixed to $n=14$, other structural variables, i.e. the structure of the perfluorinated segment and the length of the alkyl spacer group, have been varied to understand their influence on LC phase formation. These structural factors are also crucial.

2. Materials

The chemical structures of the investigated materials are shown in scheme 1. The homologous series of polycatenar materials (abbreviation: ***n*PC$_5$F^a**) have varying lengths of peripheral alkyl chains n (n=4, 6, 8, 10, 12, 14, 16) with a bulky perfluorinated part (**F^a**) and a spacer group of –O(CH$_2$)$_m$COO– (m=5). The compound having no perfluorinated moiety, **14PCR**, is an alkyl chain analogue to **14PC$_5$F^a**, while in the material **14PC$_5$F^b** an end-branched perfluorinated chain (**F^b**) is incorporated. The substance **14PC$_4$F^a** has a spacer group of –O(CH$_2$)$_m$COO– (m=4), which is one methylene unit shorter than that of **14PC$_5$F^a** (m=5). When investigating the LC phase behaviour of ***n*PC$_5$F^a**, the role of the peripheral alkyl chains will be clarified. Comparing **14PC$_5$F^a**, **14PCR** and **14PC$_5$F^b**, the influence of the perfluorinated moiety on LC phase formation will be recognized. The observed difference in mesomorphism between **14PC$_5$F^a** and **14PC$_4$F^a** will illustrate the significant role of the spacer group.

3. Synthesis

All the polycatenar materials with a perfluorinated moiety, abbreviated to ***n*PC$_m$F^{a,b}**, were prepared according to the synthesis route shown in scheme 2. Either of commercially available substances HO–**F^{a,b}** was used to incorporate a (semi)perfluorinated moiety in the materials:

$$\left[\begin{array}{l} -F^a = -\mathrm{CH_2CF(CF_3)OCF_2CF(CF_3)OCF_2CF_2CF_3;} \\ -F^b = -\mathrm{CH_2CH_2CF_2CF_2CF_2CF_2CF(CF_3)CF_3} \end{array}\right].$$

Starting from either ω-bromohexanoic acid (m=5 series) or ω-bromopentanoic acid (m=4 series), the corresponding acid chloride was made by use of thionyl chloride, which led to the ester **1$_m$F^{a,b}** by a coupling reaction with HO–**F^{a,b}**. Williamson's reaction between **1$_m$F^{a,b}** and benzyl 4-hydroxybenzoate (HOϕCOOCH$_2$ϕ) gave **2$_m$F^{a,b}**, which was hydrogenated under slight pressure of hydrogen (H$_2$) using palladium on activated charcoal (Pd/C) to yield **3$_m$F^{a,b}**. Using dicyclohexylcarbodiimide (DCC) and a small amount of

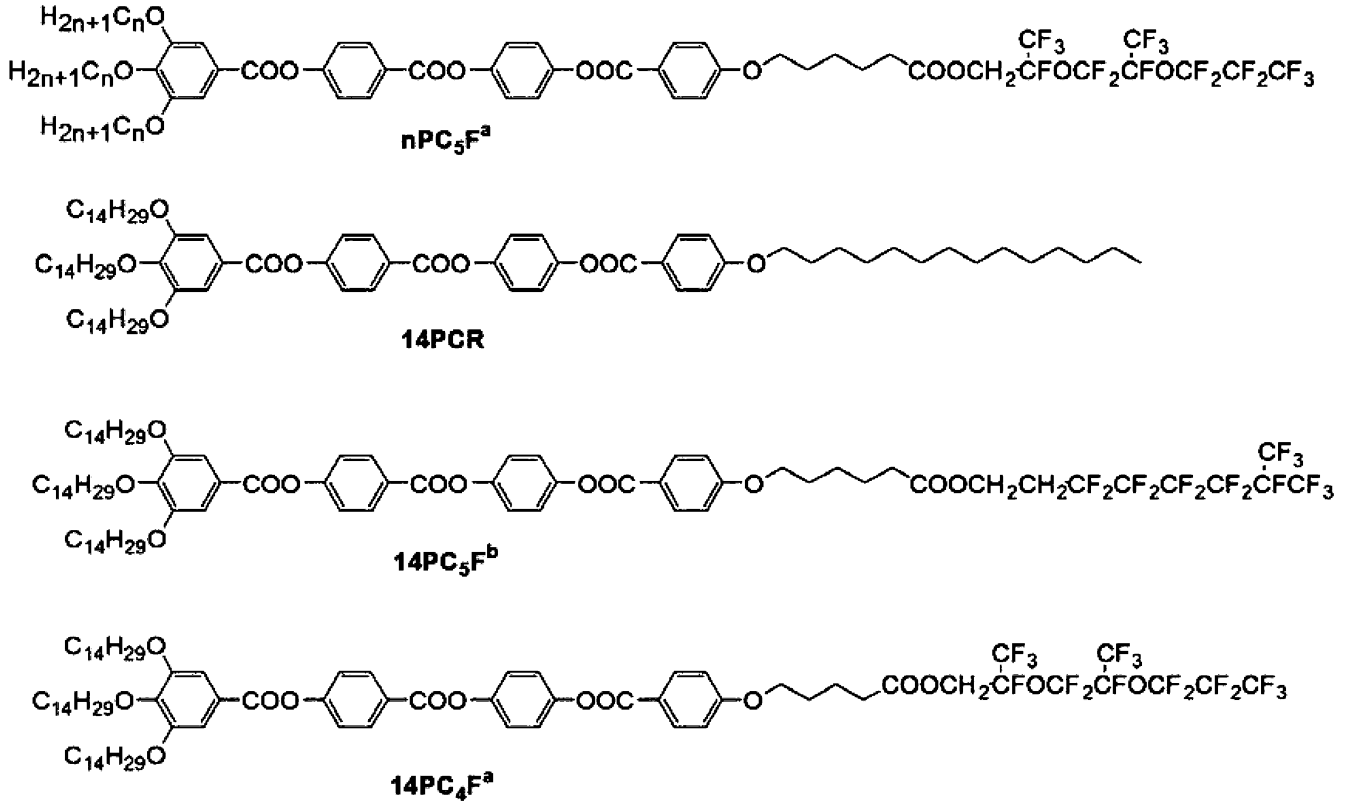

Scheme 1. Chemical structures of the polycatenar materials under investigation.

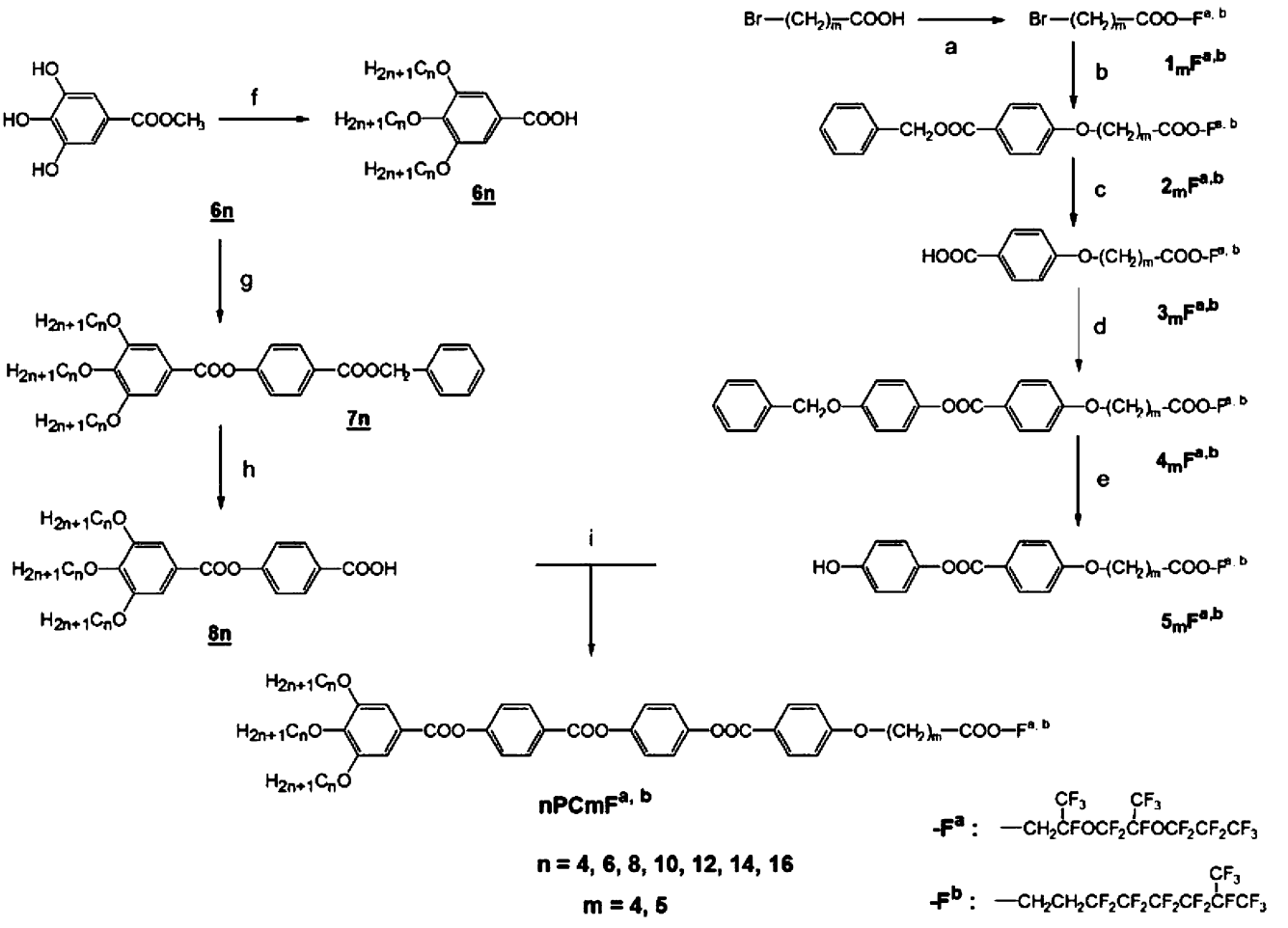

Reagent: a-1) $SOCl_2$; a-2) $F^{a,b}$-OH, Et_3N, chloroform/THF; b) HOϕCOOCH$_2$ϕ, DCC/DMAP, chloroform/THF; c) H_2/Pd-C, ethanol/ethyl acetate; d) HOϕOCH$_2$ϕ, DCC/DMAP, chloroform; e) H_2/Pd-C, ethanol/ethyl acetate; f-1) K_2CO_3, C_nH_{2n+1}-Br, acetone; f-2) KOH, ethanol/H_2O; f-3) HCl; g) HOϕCOOCH$_2$ϕ, DCC/DMAP, chloroform; h) H_2/Pd-C, ethanol/ethyl acetate; i) DCC/DMAP, chloroform

Scheme 2. Synthetic route to the polycatenar materials $n\mathbf{PC}_m\mathbf{F}^{a,b}$.

dimethylaminopyridine (DMAP), condensation between $\mathbf{3}_m\mathbf{F}^{a,b}$ and 4-benzyloxyphenol (HOϕOCH$_2$ϕ) yielded $\mathbf{4}_m\mathbf{F}^{a,b}$, which was hydrogenated to the phenol segment $\mathbf{5}_m\mathbf{F}^{a,b}$[32]. Methyl 3,4,5-trihydroxybenzoate was alkylated with an *n*-bromoalkane, and successive saponification gave the organic acids ***6n***. Condensation between ***6n*** and benzyl 4-hydroxybenzoate led to the benzyl precursors ***7n***. Deprotection of the benzyl group gave the acid segments ***8n***. Coupling reactions between $\mathbf{5}_m\mathbf{F}^{a,b}$ and ***8n*** using DCC and DMAP yielded the final polycatenar products $n\mathbf{PC}_m\mathbf{F}^{a,b}$. The chemical structures of the materials were assigned from elemental analysis, ^{1}H NMR and mass-spectrometry; details are summarized in the Experimental section together with synthetic procedures.

4. Results and discussion

We first describe the LC phase behaviour of the homologous series of polycatenar materials $n\mathbf{PC}_5\mathbf{F}^{a}$, which are composed of three peripheral alkyl chains of length n=4, 6, 8, 10, 12, 14, 16, a methylene spacer of length m=5 and the bulky perfluorinated part $\mathbf{F}^{a}$. The mesomorphism of two other materials $\mathbf{14PC}_5\mathbf{F}^{b}$ (n=14, m=5 and $\mathbf{F}^{b}$=the end-branched perfluorinated chain) and $\mathbf{14PC}_4\mathbf{F}^{a}$ (n=14, m=4 and $\mathbf{F}^{a}$=the bulky perfluorinated chain) are then discussed in comparison with the mesomorphism of $\mathbf{14PC}_5\mathbf{F}^{a}$ ($n\mathbf{PC}_5\mathbf{F}^{a}$ with n=14). The LC phase behaviour was determined by polarizing optical microscopy (POM), differential scanning calorimetry (DSC) and powder X-ray diffraction (XRD).

4.1. *LC phase behaviour of the homologues nPC$_5$F^a: the role of the peripheral alkyl chains*

The homologues ***n*PC$_5$F^a** are found to show a rich mesomorphism strongly dependent on the carbon number n of the peripheral alkyl chains.

4.1.1. 4PC$_5$F^a and 6PC$_5$F^a. The materials **4PC$_5$F^a** and **6PC$_5$F^a** show only one liquid crystalline phase, a smectic C (SmC) phase. **4PC$_5$F^a**, having three short butyloxy chains (n=4), melted to a SmC phase at 74.4°C, which transformed to an isotropic (I) liquid at 109.6°C with an enthalpy change (ΔH) of 3.5 kJ mol^{-1}. On cooling, the SmC phase formed at 109°C, where the formation of bâtonnets was observed under POM, which coalesced to a fan-shaped texture. The SmC phase was supercooled untill crystallization occurred at 54°C. An XRD intensity profile taken at 90°C in the SmC phase of **4PC$_5$F^a** exhibited first order (q_1=1.7 nm^{-1}) and second order (q_2=3.4 nm^{-1}) small angle reflections with remarkably weak intensities, comparable to that of wide angle reflections. Diele *et al.* also reported that on perfluorinated, swallow-tailed mesogens, small angle reflections with weak intensities were observed [26]. The measured layer separation of d ($=2\pi/q$)=3.7 nm was substantially shorter than the calculated molecular length l=4.5 nm, which indicates tilting of the molecules within the smectic layers. The observation of the second order reflection means that the lamellar structure is well micro-segregated. Moreover a broad weak reflection was seen around $q\sim$7 nm^{-1}, which is probably related to the segregation of the perfluorinated moieties [26, 27, 33].

6PC$_5$F^a (n=6), with three hexyloxy, groups showed an I–SmC phase transition at 81.1°C on cooling, where bâtonnets formed, growing to a fan-shaped texture. This was a similar observation to that of **4PC$_5$F^a**. On further cooling, no crystallization was observed, so the material remained as a smectic C glass. On heating, however, crystallization occurred at around 20°C, then melting into the SmC phase took place at 33°C; this was followed by the SmC–I phase transition at 81.5°C with ΔH=2.6 kJ mol^{-1}.

4.1.2. 8PC$_5$F^a and 10PC$_5$F^a. On increasing the alkyl chain length to n=8 (**8PC$_5$F^a**) and n=10 (**10PC$_5$F^a**), the phase behaviour changes. Both materials organize into two LC phases, a columnar (Col) phase and a smectic A (SmA) phase.

8PC$_5$F^a melted at 62.2°C into a Col phase and transformed to a SmA phase at 72.4°C with ΔH=0.87 kJ mol^{-1}. An isotropic phase transition then occurred at 90.9°C with ΔH=0.68 kJ mol^{-1}. On cooling, the material exhibited the same phase sequence. POM observations showed a uniform homeotropic orientation in the SmA phase between non-coated glass plates. The Col phase, which has low fluidity, shows a grain-like texture with weak birefringence. XRD patterns of these LC phases are shown in figure 1. In the SmA phase a strong small angle reflection at q=0.82 nm^{-1} is observed, corresponding to a d-spacing of 7.6 nm; the calculated molecular length is about 5.23 nm. Thus a partially interdigitated SmA phase may be indicated. In the Col phase at 70°C the XRD pattern appears to exhibit one considerably broad, strong small angle reflection, which can be analysed as the overlapping of two peaks at q_1=0.87 nm^{-1} and q_2=0.94 nm^{-1}, as shown with dotted lines. It may be possible to assign rectangular symmetry to the Col phase. Further detailed investigation would be necessary to determine clearly the nature of the low temperature phase.

10PC$_5$F^a melted at 62.7°C into a Col phase, followed by SmA formation at 68°C. The Col–SmA transition was observed with POM, but not DSC. A SmA–I transition then occurred at 105.7°C with ΔH=0.35 kJ mol^{-1}. On cooling, the same phase behaviour was observed. In figure 2 the XRD patterns of the LC phases are shown. The SmA phase shows a small angle reflection at q=0.79 nm^{-1}, while an XRD pattern of the Col phase exhibits a set of small angle reflections at q_1=0.53, q_2=0.85 and q_3=1.07 nm^{-1}; the ratio q_1:q_2:q_3, however, corresponds neither to a tetragonal (1:2$^{1/2}$:2) nor a hexagonal symmetry (1:3$^{1/2}$:2).

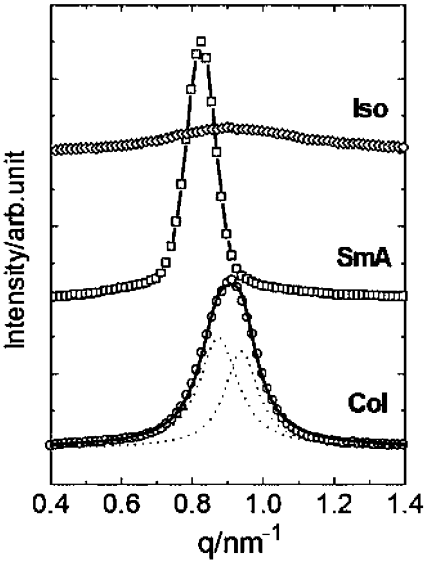

Figure 1. XRD patterns at small angle regions of **8PC$_5$F^a** observed (◇) in the isotropic phase, (□) in the smectic A phase and (○) in the columnar phase.

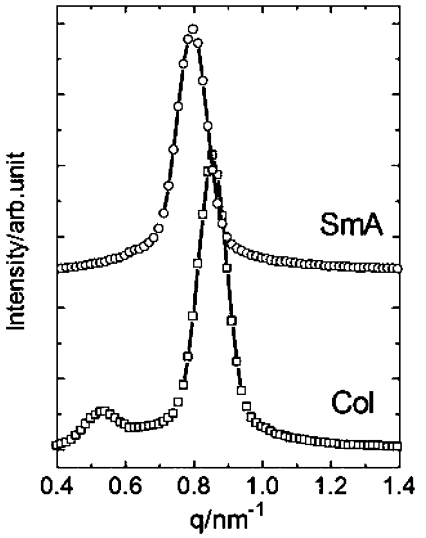

Figure 2. XRD patterns at small angle regions of **10PC$_5$F^a** observed (○) in the smectic A phase and (□) in the columnar phase.

4.1.3. 12PC$_5$F^a and 14PC$_5$F^a. In previous work we reported that the polycatenar material **14PC$_5$F^a** (**14PCF**; the previous abbreviation) showed the trimesomorphism of a cubic phase, a columnar phase and a smectic A phase, as a function of temperature [30, 31]. However, reinvestigation of the material has revealed that its LC phase behaviour, which we describe here, is more complicated. In figure 3 DSC data of **14PC$_5$F^a** are shown. On the first heating, three endothermic peaks at about 47, 54 and 64°C were observed, while on the second heating the endothermic peak at 64°C did not appear. This means that the crystals obtained from solution are different from the crystalline form from the melt. On second heating the formation of three LC phases was detected (see the inset of figure 3).

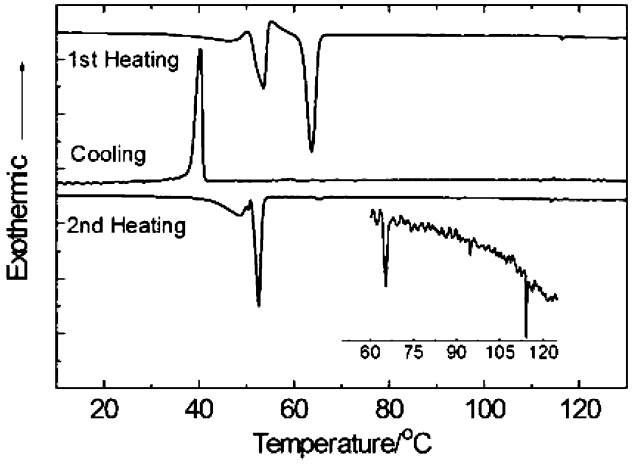

Figure 3. DSC chart of **14PC$_5$F^a** measured at a heating/cooling scanning rate of 2°C min^{-1}.

POM observation confirmed three LC phases, as shown in figure 4. On heating, a crystalline phase (*a*) transformed to an optically extinct phase at 52.6°C (*b*), which could possibly be a cubic phase. Then a birefringent LC phase (columnar) appeared at 65.3°C (*c*), which transformed to a SmA phase at 94.2°C, followed by an isotropic phase transition at 115°C. On cooling in the SmA phase homeotropic alignment was seen, as shown in figure 4 (*d*). Thereafter the Col phase appeared at 94°C, where its characteristic texture was observed, figure 4 (*e*); this Col phase transformed to a weakly birefringent LC phase at 59°C as shown in figure 4 (*f*). At first we assigned this low temperature phase to a cubic phase with some remaining birefringent regions of the supercooled Col phase [30, 31]. However, the texture did not change further, even after long annealing. Now we suppose this phase to be an ordered columnar phase. Eventually crystallization took place at 40.3°C.

These observations indicate that the low temperature LC phases formed during cooling or heating could be different, or the LC phase formed on heating could also be a columnar phase even though no birefringence was observed. Note that on annealing, crystallization gradually took place in the low temperature LC phase formed on heating; it is thus a metastable phase. XRD patterns of all the LC phases are shown in figure 5. In the SmA phase one sharp small angle reflection at $q=0.77\,\mathrm{nm}^{-1}$ ($q=4\pi\sin\theta/\lambda$; 2θ=scattering angle; $\lambda=0.154\,\mathrm{nm}$) was seen; that is, $d=8.16\,\mathrm{nm}$, which indicates a partially interdigitated SmA phase. In the Col phase three reflections were observed, their $1{:}2^{1/2}{:}2$ ratio revealing a tetragonal symmetry. The XRD pattern of the low temperature mesophase formed on heating appeared to be slightly different from that formed on cooling, which also indicates the possibility of different LC phase formations. No Bragg-like spot reflections were observed for either form, which shows that the low temperature LC phase is probably not a cubic phase; we have no further conclusions for this phase.

The LC phase behaviour of **12PC$_5$F^a** is the same as that of **14PC$_5$F^a**. On heating, the crystalline phase of **12PC$_5$F^a** melted into a non-birefringent LC phase at 51.6°C. Then a Col phase formed at 62.9°C with $\Delta H=0.24\,\mathrm{kJ\,mol}^{-1}$; this was followed by transition into a SmA phase at 74.2°C with $\Delta H=0.16\,\mathrm{kJ\,mol}^{-1}$. A SmA–I phase transition then took place at 113.5°C with $\Delta H=0.35\,\mathrm{kJ\,mol}^{-1}$. During cooling below the SmA and Col phases, a weakly birefringent phase was observed, which is possibly an ordered Col phase. XRD intensity

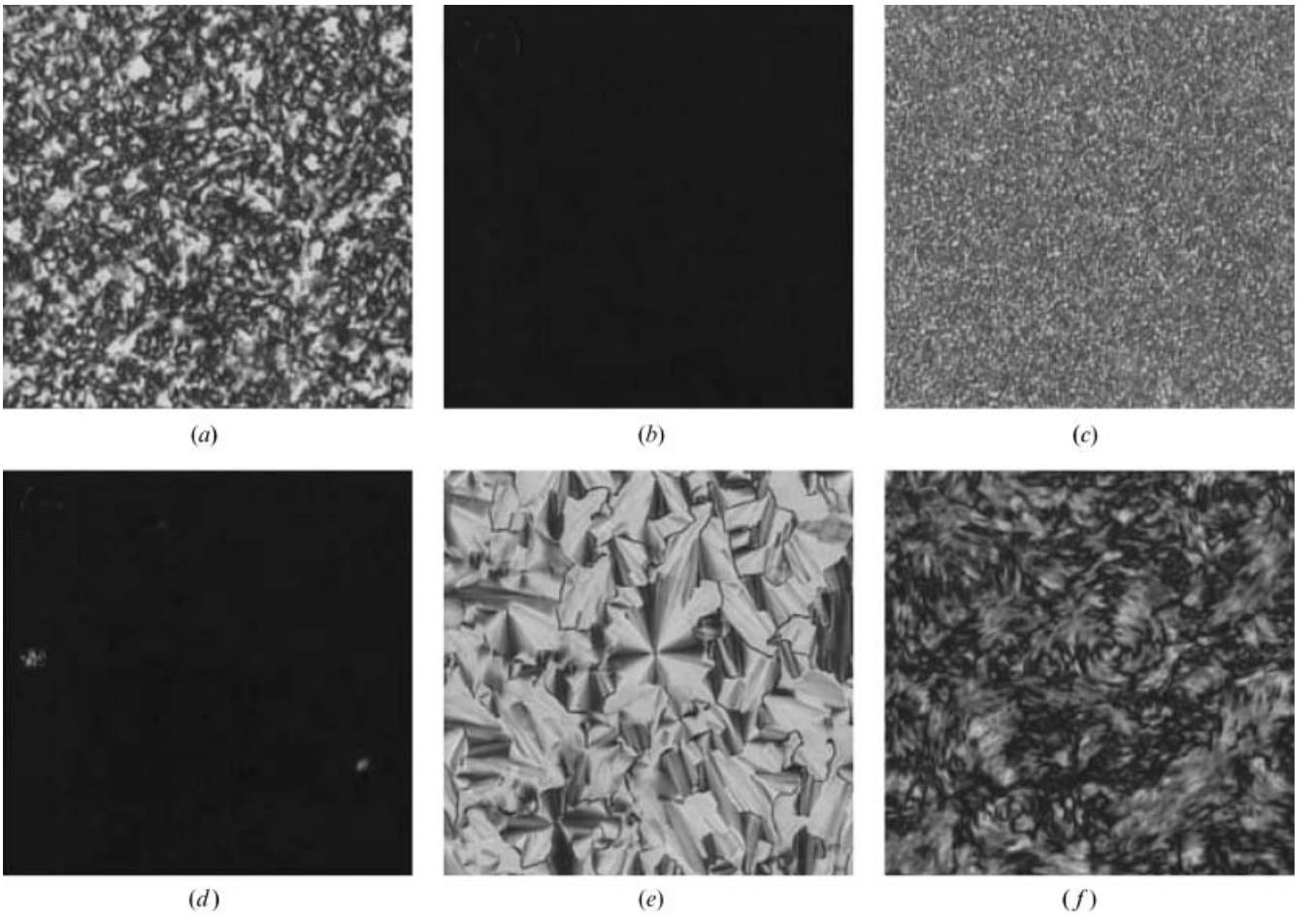

Figure 4. POM pictures of **14PC$_5$F^a** observed (*a*) in the crystalline phase, (*b*) in the low temperature LC phase, (*c*) in the columnar phase on heating, (*d*) in the smectic A phase, (*e*) in the columnar phase, (*f*) in the low temperature LC phase on cooling.

profiles of the mesophases of **12PC$_5$F^a** are similar to those of **14PC$_5$F^a**. In the SmA phase at 110°C a small angle reflection at $q=0.78\,\mathrm{nm}^{-1}$ was observed, which corresponds to a layer separation of 8.1 nm. In the Col phase at 70°C, three small angle reflections at $q_1=0.54$, $q_2=0.83$ and $q_3=1.06\,\mathrm{nm}^{-1}$ were observed. The ratio $q_1{:}q_2{:}q_3$ correlates closely with the theoretical $1{:}2^{1/2}{:}2$ of tetragonal symmetry. The XRD patterns of the low temperature LC phases formed on cooling and heating were slightly different; the reason for this is not completely understood.

4.1.4. 16PC$_5$F^a. On increasing further the length of peripheral alkyl chains, we obtain the hexadecyloxy homologue **16PC$_5$F^a** ($n=16$), which is found to exhibit columnar phases but no lamellar phase. On cooling from the isotropic phase, a spherulitic texture was observed at 125°C with POM, which clearly indicates the formation of a Col phase (high temperature columnar phase: Col$_H$). DSC measurements observed the Col$_H$–I phase transition with ΔH of $0.49\,\mathrm{kJ\,mol}^{-1}$, as shown in figure 6. On further cooling, although the texture appeared not to change significantly and no peak was detected with DSC, a Col$_H$ to a Col$_M$ (middle temperature columnar) phase transition was found to take place at about 98°C, as described below from XRD results. Then at about 62°C the texture clearly changed, showing weak birefringence, which reveals a Col$_L$ (low temperature columnar) phase formation; this transition was detected by DSC. Crystallization (into Cr$_1$) then took place at 52.4°C.

On heating, an exothermic peak was observed at 61.2°C, indicating crystallization (into Cr$_2$). This process was found to occur kinetically slowly; for example, under POM observation, several minutes were needed for complete crystallization. This crystal (Cr$_2$) melted at 75.1°C into a Col$_M$ phase; no Col$_L$ phase was observed. However, at a fast scanning rate, which prevented complete crystallization to Cr$_2$, the remaining crystal phase (Cr$_1$) transformed into a very weak

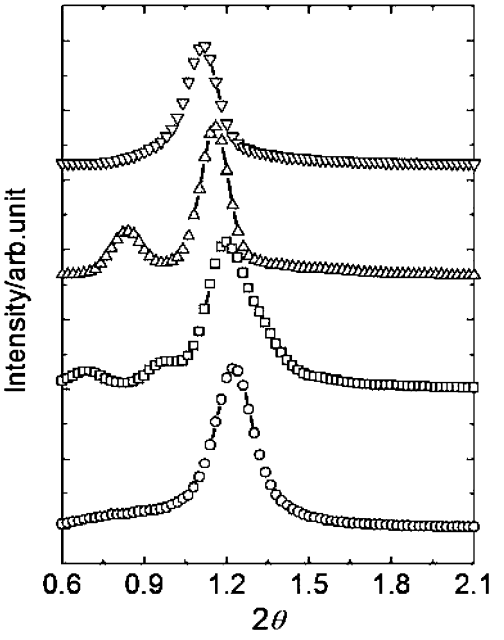

Figure 5. XRD patterns of **14PC$_5$F^a** observed (▽) in the smectic A phase, (△) in the tetragonal columnar phase, (□) in the low temperature LC phase on cooling and (○) in the low temperature LC phase on heating.

birefringent phase, which was probably an indication of a Col_L phase. No Col_M–Col_H phase transition was observed by either POM or DSC. The Col_H–I phase transition occurred at 125°C with ΔH of 0.46 kJ mol^{-1}.

Figure 7 shows XRD intensity profiles observed for the LC phases of **16PC$_5$F^a**. In the I phase a diffuse small angle reflection was observed, which means that a micro-separated structure exists even in the optically isotropic phase. On cooling into the Col_H phase, several discrete Bragg-like spots were observed at small angles, showing weak orientation of the Col_H phase in a glass

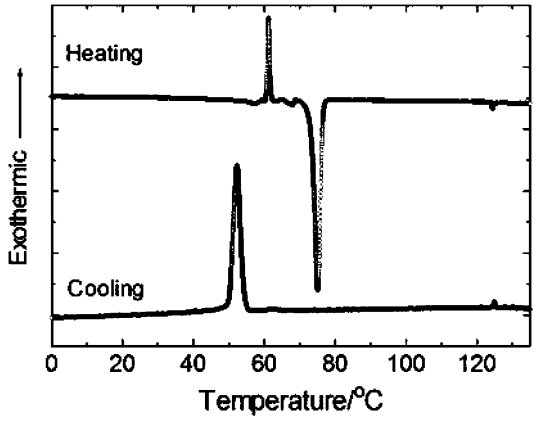

Figure 6. DSC chart of **16PC$_5$F^a** obtained at a heating/cooling scanning rate of 2°C min^{-1}.

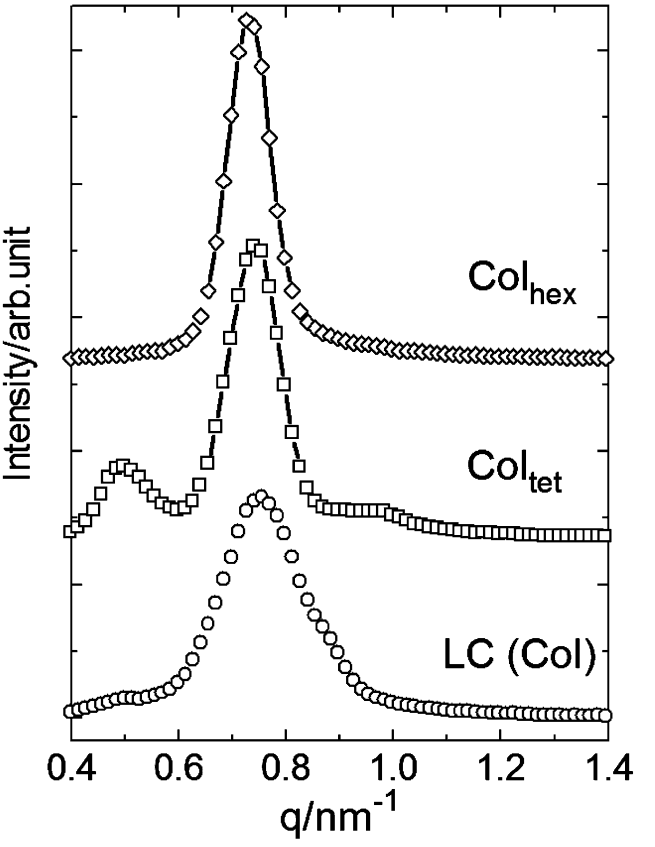

Figure 7. XRD patterns of **16PC$_5$F^a**, observed (◇) in the high temperature hexagonal columnar phase, (□) in the middle temperature tetragonal columnar phase and (○) in the low temperature columnar phase.

tube. The intensity profile appears to show only one small angle reflection at q=0.73 nm^{-1}, which indicates a hexagonal columnar phase with weak correlation among the columns. The unit cell parameter was calculated as a=10 nm according to the relationship $a=(2/3^{1/2})d_{10}$ with $d_{10}=2\pi/q$. On further cooling, the XRD pattern changed at about 98°C, showing the formation of another phase, the Col_M phase. An XRD intensity profile in the Col_M phase showed three reflections at q_1=0.50, q_2=0.74 and q_3=0.99 nm^{-1}. The ratio q_1:q_2:q_3 closely corresponding to the ratio 1:2$^{1/2}$:2, indicates the Col_M phase to have a tetragonal symmetry. Therefore, a hexagonal to tetragonal columnar phase transition takes place in this material. The unit cell parameter of the tetragonal Col_M phase was calculated as a=12.0 nm, which is larger than the unit cell parameter of the hexagonal Col_H phase of a=10 nm. On cooling from the Col_M phase, the XRD pattern substantially changed. The intensity profile at 57°C showed very broad (overlapped) small angle reflections, revealing the formation of the Col_L phase. We have not completely identified the symmetry.

Table. Phase transition temperatures (°C) and enthalpy changes (kJ mol^{-1} in italics): n is the carbon number of the peripheral alkyl chains of ***n*PC$_5$F^a**; Cr=crystalline, SmC=smectic C, LC=liquid crystalline, Col=columnar, SmA=smectic A, I=isotropic.

n	Cr		SmC		LC		Col		SmA		I
4	•	74.4	•	109.6	—		—		—		•
		12.9		*3.5*							
6	•	32.9	•	81.5	—		—		—		•
		14.1		*2.6*							
8	•	62.2	—		—		•	72.4	•	90.9	•
		17.8						*0.87*		*0.68*	
10	•	62.7	—		—		•	68	•	105.7	•
		19.1						—		*0.35*	
12	•	51.6	—		•[a]	62.9	•	74.2	•	113.5	•
		36.2				*0.24*		*0.16*		*0.35*	
14	•	52.6	—		•[a]	65.3	•	94.2	•	115	•
		28.1				*0.6*		*0.07*		*0.34*	
16	•	75.1	—	(Cr 52	•	62)[b]	•[c]		—	124.5	•
		56								*0.46*	

[a]The LC phase is not completely identified. [b]Monotropic phase transition into an ordered Col phase. [c]A hexagonal to tetragonal columnar phase transition was observed about 98°C.

4.1.5. The homologues. The phase behaviour of the homologous series of polycatenar compounds ***n*PC$_5$F^a** is summarized in table 1 and figure 8. When the length of peripheral alkyl chains is short (n=4, 6), only a SmC phase forms. The formation of a SmC phase has often been observed in polycatenar mesogens with short peripheral chain homologues [8]. On increasing the chain length to n=8, 10, a no SmC phase formation occurs; instead a Col phase and a SmA phase are observed. On further increasing the length of peripheral chains to n=12, 14, another LC phase is formed at lower temperature. The polycatenar mesogen with the longest peripheral chains under study (n=16) forms hexagonal and tetragonal Col phases and another monotropic, Col phase at lower temperature. Lamellar phase formation disappears. These results prove the significant role of the peripheral alkyl chain length in the organization of LC phases.

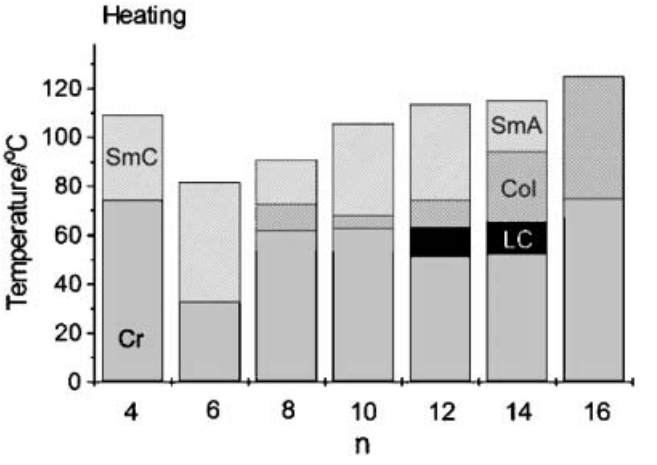

Figure 8. Liquid crystalline phase behaviour of the homologous series of polycatenar materials ***n*PC$_5$F^a** (n=the number of carbon atoms of the peripheral alkyl chains).

4.2. *The LC phase behaviour of* **14PC$_5$F^b***: the role of the perfluorinated group*

The previous section has clearly shown the important role of the peripheral alkyl chains of the polycatenar materials in the formation of LC phases. Here the role of the perfluorinated segment is described. The presence of a perfluorinated segment was recognized to be essential after synthesizing the polycatenar material **14PCR**, having no perfluorinated moieties, which exhibited no LC phases. The material melted at 72°C to an isotropic liquid.

When a different perfluorinated moiety is used instead of the **F^a** of **14PC$_5$F^a**, the LC phase behaviour can be changed; this was studied with **14PC$_5$F^b**, having the end-branched perfluorinated chain **F^b**. DSC measurements showed the formation of two LC phases on both cooling and heating; POM observations confirmed two LC phases. Two photomicrographs obtained with POM are shown in figure 9. On heating, the material transformed into a LC phase at 71.2°C showing no birefringence, i.e. a Cub phase, which transformed to a Col phase at 93.6°C with an enthalpy change of 1.0 kJ mol^{-1}. An isotropic phase transition then occurred at 107°C with ΔH of 0.59 kJ mol^{-1}. On cooling, the Col phase appeared at 106.3°C with a characteristic spherulitic texture, figure 9 (*a*). The texture changed at 92.2°C with the birefringence beginning to disappear, figure 9 (*b*); crystallisation took place at 37.9°C. The microstructure of the LC phases was

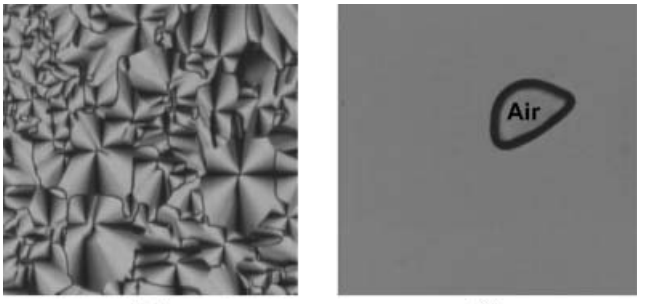

Figure 9. POM photomicrographs of **14PC$_5$F^b** (*a*) in the columnar phase and (*b*) in the cubic phase.

investigated with XRD; the intensity profile observed in the Col phase is shown in figure 10 (*a*), which indicates a hexagonal Col phase (Col_{hex}), instead of the previously described tetragonal Col phase. At lower temperature the XRD pattern changed to the complex pattern shown in figure 10 (*b*), indicative of the formation of a Cub phase.

Compared with the compound **14PC$_5$F^a**, which forms three LC phases, **14PC$_5$F^b** has been found to exhibit considerably different LC phase behaviour. This result

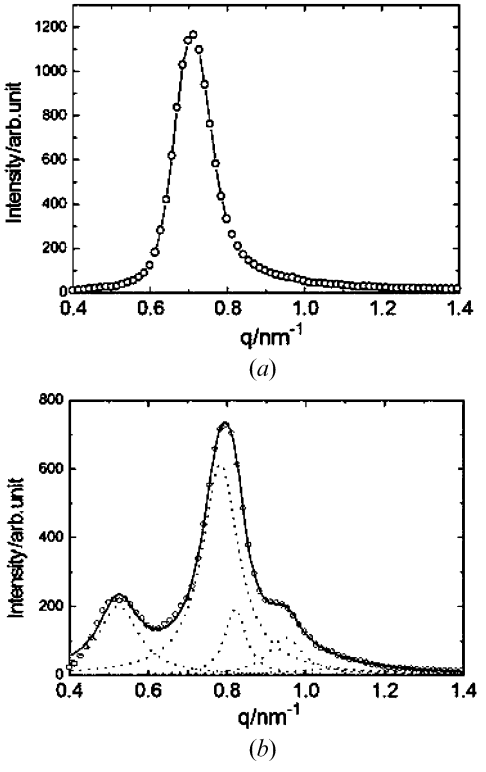

Figure 10. XRD patterns of **14PC$_5$F^b** observed (*a*) in the columnar phase and (*b*) in the cubic phase.

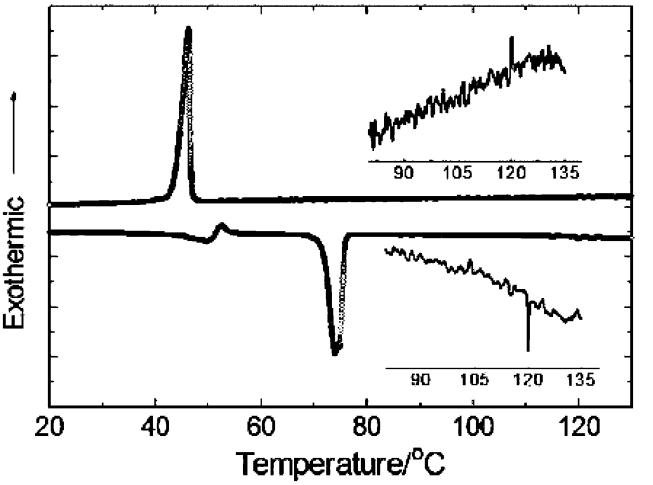

Figure 11. DSC chart of **14PC$_4$F^a** obtained at a heating/cooling scanning rate of 2°C min^{-1}.

shows that the structure of the perfluorinated moiety has a significant influence on the LC phase formation.

4.3. *The LC phase behaviour of* 14PC$_4$F^a*: the role of the spacer group*

In this section we discuss another structural factor, namely the incorporation of spacer group $–O(CH_2)_mCOOCH_2–$ that separates the chemically different perfluorinated and hydrocarbon moieties. The polycatenar material **14PC$_4$F^a** has the spacer $–O(CH_2)_4COOCH_2–$ (m=4) that is one methylene unit shorter than the spacer $–O(CH_2)_5COOCH_2–$ (m=5) of **14PC$_5$F^a**.

Figure 11 shows a DSC thermogram of **14PC$_4$F^a**; the I to LC phase transition was observed at 120°C on both heating and cooling, with a small enthalpy change of about 0.2 kJ mol^{-1}. Melting occurred at *c*. 75°C with ΔH=65 kJ mol^{-1} (note that double meltings were observed), while the LC phase supercooled to crystallize at about 45°C. Although only one LC phase was found with DSC, POM observations revealed three kinds of LC phase. On cooling from the isotropic liquid a spherulitic texture was observed at 120°C, as shown in figure 12 (*a*), which shows that a high temperature columnar (Col_H) phase is formed. At 112°C the texture became dark, indicating a phase transition, see figure 12 (*b*). The dark areas of the picture indicate homeotropic orientation, and oily-streaks were observed in the fluid phase, which is assigned as smectic A. On further cooling, a characteristic texture again appeared at 99°C, as shown in figure 12 (*c*), which indicates an organization into a low temperature columnar (Col_L) phase. As neither the Col_H–SmA or

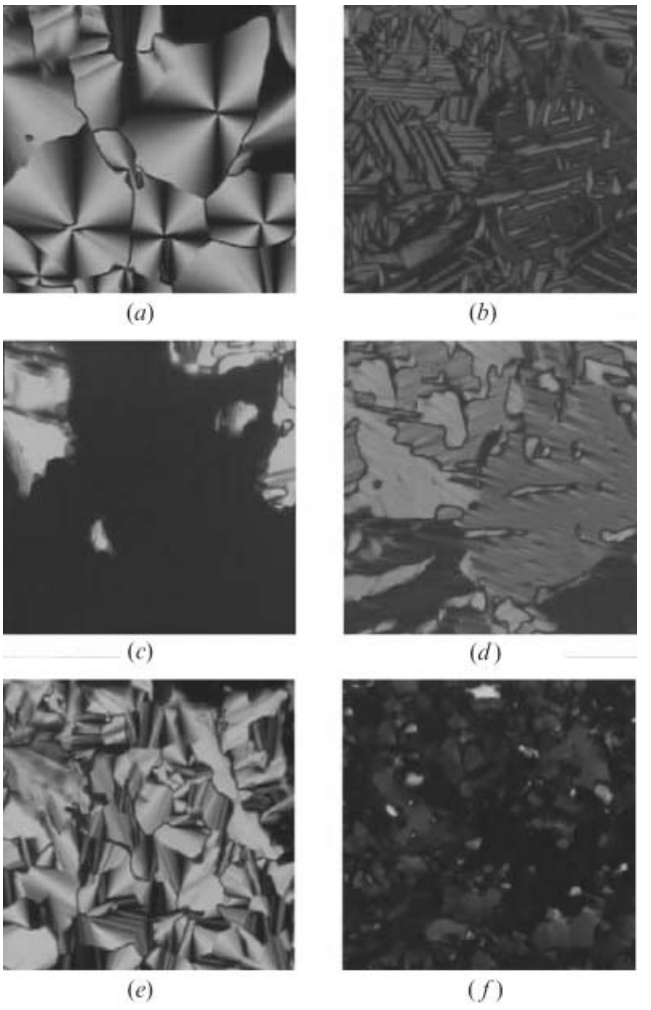

Figure 12. POM photomicrographs of **14PC$_4$F**[a] observed between two normal glass plates (*a*) at 120°C in the hexagonal columnar (Col_{hex}) phase, (*b*) at 110°C in the SmA phase, (*c*) at 99°C in the tetragonal columnar (Col_{tet}) phase; and between two polyimide-coated glass plates (*d*) at 115°C in the Col_{hex} phase, (*e*) at 101°C in the SmA phase, (*f*) at 94°C in the Col_{tet} phase.

SmA–Col_L phase transitions were detected with DSC, these are probably of second order. When sandwiched between two polyimide-coated glass plates, the compound also exhibited distinct textures for the three LC phases; these are shown in figure 12 (*d*) corresponding to the Col_H phase, 12 (*e*) to the SmA phase showing planar orientation, and 12 (*f*) to the Col_L phase, respectively. The three kinds of mesophase were also found to form on heating.

The microstructure of the LC phases was studied with XRD. figures 13 (*a–c*) present the XRD patterns observed at 118°C in the Col_H phase, at 106°C in the SmA phase and at 90°C in the Col_L phase, respectively. In the Col_H phase the small angle reflection pattern

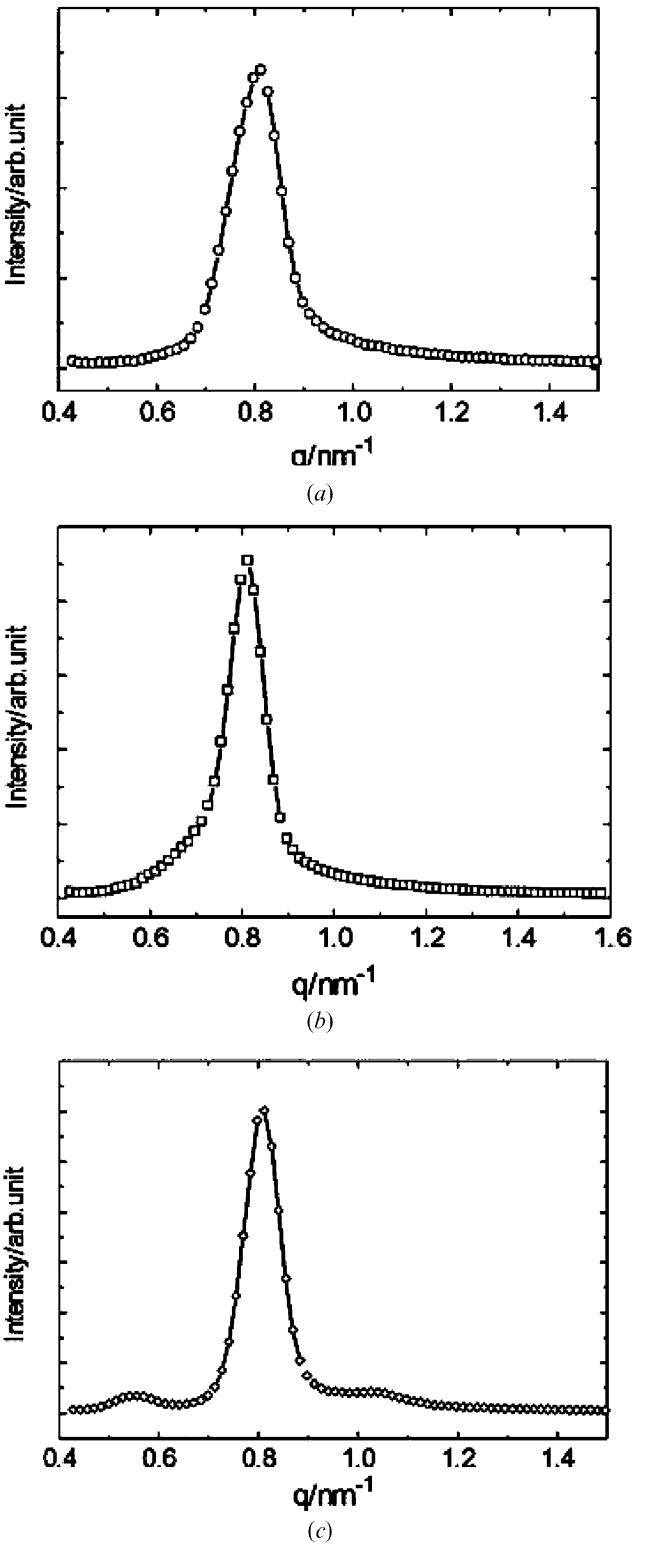

Figure 13. XRD patterns of **14PC$_4$F**[a] observed (◇) at 118°C in the hexagonal columnar phase, (□) at 106°C in the smectic A phase and (○) at 90°C in the tetragonal columnar phase.

exhibits only one peak at $q=0.803\,nm^{-1}$. No high order reflections were observed, which shows the Col_H phase to be hexagonal (Col_{hex}) with weak correlation of the columns. In the SmA phase a small angle reflection was observed at $q=0.807\,nm^{-1}$ (layer separation of $d=2\pi/q=7.78\,nm$). The molecular length is about 5.9 nm, thus an interdigitated smectic A phase may be supposed. In the Col_L phase the small angle reflection pattern showed three peaks at $q_1=0.542$, $q_2=0.807$ and $q_3=1.07\,nm^{-1}$, whose ratio corresponds to $1:2^{1/2}:2$, thus indicating a two-dimensional tetragonal columnar (Col_{tet}) phase with a lattice constant of 11.5 nm. It has therefore been concluded that the polycatenar material shows the three enantiotropic LC phases, Col_{tet}, SmA and Col_{hex}, as a function of temperature. This LC phase sequence is considerably different from that of **14PC$_5$F^a**, therefore this result has shown that a slight change of molecular structure, by one methylene unit in the spacer group (note the change of parity), causes a remarkable change in the mesophase formation. In other words, the spacer group of the polycatenar mesogens plays a crucial role in the formation of LC phases.

5. Conclusions

Polycatenar materials composed of a four-aromatic-ring core with a bulky or end-branched perfluorinated moiety attached at one end through a spacer group, and three peripheral alkyl chains of varying length substituted on the other end-ring, were synthesized and their LC phase behaviour investigated.

The study of the homologous series of polycatenar materials ***n*PC$_5$F^a** (the carbon number of the alkyl chains $n=4$, 6, 8, 10, 12, 14, 16) demonstrated the important role of the peripheral alkyl chains in LC phase formation. It was found that homologues with short peripheral chains ($n=4$, 6) formed a smectic C phase. The octyloxy- ($n=8$) and decyloxy- ($n=10$) homologues formed columnar and smectic A phases, but no SmC phase. The homologues with $n=12$ and 14 exhibited three mesophases, a non-identified LC phase, a tetragonal columnar phase and a SmA phase, as a function of temperature. On increasing the chain length to $n=16$, the resulting material did not form lamellar phases but organized into three columnar phases.

The presence and chemical structure of the perfluorinated moiety, and the presence and length of the spacer group, remarkably affected mesophase formation. One material was found to show a unique LC phase sequence: hexagonal columnar – smectic A – tetragonal columnar.

This study has shown that the class of polycatenar materials containing a perfluorinated moiety exhibits rich mesomorphism due to striking steric and chemical molecular features.

6. Experimental

6.1. *Measurements*

The chemical structures of the synthesized compounds were assigned by elemental analysis, ^{1}H NMR spectrometry and mass (MS) spectrometry. ^{1}H NMR spectra were observed on a Bruker DRX500 NMR-spectrometer using d-chloroform as solvent and tetramethylsilane as internal standard (see scheme 3 for designation of aromatic protons). MS spectra were obtained on a Joel, JMS-700 instrument using the FD/MS method.

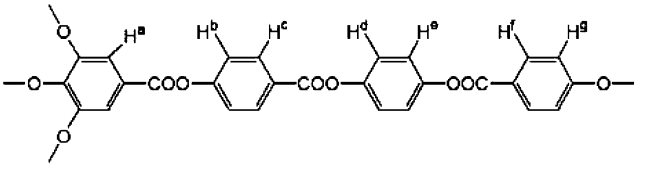

Scheme 3. Designation of aromatic protons in ^{1}H NMR.

DSC data were obtained on a Mac Science DSC-3100 instrument at a heating/cooling scan rate of $2^\circ C\,min^{-1}$ using about 10 mg of sample. POM was performed on an Olympus BX-50 microscope equipped with a Linkam hot stage LK-600PH. XRD patterns were observed using monochromatic Cu-K_α radiation of wavelength 0.154 nm from a 1.6 kW X-ray generator; a two-dimensional position sensitive detector was used, which had 1024×1024 pixels in a $15\times15\,cm^2$ beryllium window.

6.2. *Synthesis*

6.2.1. 4-{5-[1H,1H-2,5-di(trifluoromethyl)-3,6-dioxaundecafluorononyloxycarbonyl]pentyloxy}benzoic acid 3$_5$F^a. The synthetic procedures for the phenol segments **5$_5$F^a**, **5$_4$F^a** and **5$_5$F^b** were same, so only the synthesis of phenol **5$_5$F^a** is described. A solution of 3 g (15.4 mmol) of 6-bromohexanoic acid in 5 ml of thionyl chloride and 3 drops of dimethylformamide was stirred for 24 h at room temperature. Excess thionyl chloride was removed under vacuum and the residue dissolved in a mixture of 20 ml dry methylene chloride (CH_2Cl_2) and 5 ml dry tetrahydrofuran (THF). Under ice cooling a solution of 6.2 g (12.9 mmol) of 1H,1H-2,5-di(trifluoromethyl)-3,6-dioxaundecafluorononanol and 1.6 g of triethylamine in 20 ml CH_2Cl_2 and 5 ml THF was added dropwise over 1.5 h; the mixture was stirred overnight at room temperature. The solvent was evaporated and the residue extracted with diethyl ether (300 ml). After the precipitate was filtered off, the ether solution was washed with 10% aqueous sodium hydroxide (NaOH) and saturated aq. sodium chloride (NaCl). The organic

layer was dried over magnesium sulphate ($MgSO_4$) and concentrated to yield the crude product $\mathbf{1_5}$, which was then dissolved in 100 ml of acetone. To this solution, 3.5 g of benzyl 4-hydroxybenzoate and 8 g of potassium carbonate were added and the mixture stirred at 50°C for 3 days. The solid was filtered off and the filtrate concentrated. The residue was dissolved in ethyl ether and washed with 10% aq. NaOH and sat. aq. NaCl. The organic layer was dried over $MgSO_4$ and concentrated to obtain the crude product $\mathbf{2_5F^a}$. Purification was carried out by column chromatography using ethyl acetate/hexane=1/5 to yield 7.1 g of $\mathbf{2_5F^a}$ (57.5%). The deprotection of the benzyl group was performed in a mixture of 40 ml ethanol and 80 ml ethyl acetate using 0.71 g of Pd/C under a slight pressure of H_2 at room temperature overnight, to yield 6 g of the product $\mathbf{3_5F^a}$ (quantitative).

$\mathbf{3_5F^a}$: *m/z* 716 (M^+). Elemental analysis (%): found (calc. for $C_{22}H_{17}F_{17}O_7$) C 37.0 (36.89), H 2.5 (2.39), F 41.7 (41.09). ^{1}H NMR (δ_H/ppm, 500 MHz, $CDCl_3$); 1.53 (m, 2H, –CH_2–), 1.74 (q, 2H, –CH_2–), 1.83 (q, 2H, –CH_2–), 2.43 (t, 2H, –OOCCH_2–), 4.03 (t, 2H, –CH_2O–), 4.58–4.72 (m, 2H, –F^aCH_2–), 6.92 (d, 2H, Ar–H), 8.05 (d, 2H, Ar–H), 12 (bs, 1H, –COOH).

6.2.2. 4-Hydroxyphenyl 4-{5-{1H,1H-2,5-di(trifluoromethyl)-3,6-dioxaundecafluorononyloxycarbonyl}pentyloxy}benzoate $\mathbf{5_5F^a}$. A solution of $\mathbf{3_5F^a}$ (3 g, 5.02 mmol), 4-benzyloxyphenol (1 g, 5.02 mmol), DCC (1.04 g, 5.02 mmol) and DMAP (61 mg, 0.1 eq.) in 45 ml CH_2Cl_2 was stirred at room temperature overnight. The precipitate was filtered off and the filtrate concentrated. The residue was purified by column chromatography (ethyl acetate/hexane=1/3) to yield 2.45 g of the benzyl ester $\mathbf{4_5F^a}$ (65%); this was hydrogenated using 0.25 g of Pd/C under a slight pressure of H_2 in a solvent of ethanol and ethyl acetate to yield 2 g of the product $\mathbf{5_5F^a}$ (quantitative).

$\mathbf{4_5F^a}$: *m/z* 898 (M^+). Elemental analysis (%): found (calc. for $C_{35}H_{27}F_{17}O_8$) C 47.1 (46.8), H 2.8 (3.0), F 35.5 (36.0). ^{1}H NMR (δ_H/ppm, 500 MHz, $CDCl_3$); 1.54 (m, 2H, –CH_2–), 1.74 (q, 2H, –CH_2–), 1.85 (q, 2H, –CH_2–), 2.45 (t, 2H, –OOCCH_2–), 4.04 (t, 2H, –CH_2O–Ar), 4.65 (q, 2H, –CFCH_2–), 5.07 (s, 2H, OCH_2–Ar), 6.95 (d, 2H, Ar–H), 7.06 (dd, 4H, Ar–H), 7.33–7.46 (m, 5H, Ar–H), 8.13 (d, 2H, Ar–H). $\mathbf{5_5F^a}$: *m/z* 808 (M^+). Elemental analysis (%): found (calc. for $C_{28}H_{21}F_{17}O_8$). C 42.2 (41.6), H 2.5 (2.62), F 38.8 (39.95). ^{1}H NMR (δ_H/ppm, 500 MHz, $CDCl_3$); 1.54 (m, 2H, –CH_2–), 1.74 (q, 2H, –CH_2–), 1.85 (q, 2H, –CH_2–), 2.45 (t, 2H, –OOCCH_2–), 4.04 (t, 2H, –CH_2O–), 4.66 (q, 2H, –CFCH_2–), 6.84 (d, 2H, Ar–H), 7.00 (dd, 4H, Ar–H), 8.13 (d, 2H, Ar–H).

6.2.3. 4-[3,4,5-tri(n-alkyloxy)benzoyloxy]benzoic acids 8*n*. As all the organic acids $\mathbf{8}n$ were synthesized by the same procedure, the synthesis of $\mathbf{8_{14}}$ is described as a representative method. To a solution of 1.3 g (1.71 mmol) of the acid $\mathbf{6_{14}}$ and 0.39 g (1.71 mmol) of benzyl 4-hydroxybenzoate in 20 ml CH_2Cl_2, a solution of 0.352 g (1.71 mmol) of DCC and 21 mg (0.171 mmol) of DMAP in 5 ml CH_2Cl_2 was added and the mixture stirred at room temperature overnight. After filtration of the precipitate, the solvent was evaporated and the residue purified by column chromatography using ethyl acetate/chloroform/hexane=1/2/7 to yield 1.1 g (66%) of the product $\mathbf{7_{14}}$.

To a solution of 1 g (1 mmol) of $\mathbf{7_{14}}$ in 20 ml ethyl acetate and 10 ml ethanol, 0.1 g of Pd/C was added and the mixture stirred at room temperature overnight under a slight pressure of H_2. The solid was filtered off and the solvent evaporated to yield $\mathbf{8_{14}}$ quantitatively.

$\mathbf{7_{14}}$: *m/z* 969 (M^+). Elemental analysis (%): found (calc. for $C_{63}H_{100}O_7$) C 77.9 (78.05), H 10.50 (10.43).^{1}H NMR (δ_H/ppm, 500 MHz, $CDCl_3$): 0.88 (t, 9H, –CH_3), 1.26–1.33 (m, 60H, –CH_2–), 1.44–1.50 (m, 6H, –CH_2–), 1.72–1.86 (m, 6H, –CH_2–), 4.0–4.08 (m, 6H, –OCH_2–), 5.38 (s, 2H, –CH_2–Ph), 7.36 (dd, 2H, aromatic H), 7.35–7.47 (m, 5H, aromatic H), 7.39 (s, 2H, aromatic H), 8.16 (dd, 2H, aromatic H). $\mathbf{8_{14}}$: *m/z* 879 (M^+). Elemental analysis (%): found (calc. for $C_{56}H_{94}O_7$) C 76.3 (76.49), H 11.0 (10.78). ^{1}H NMR (δ_H/ppm, 500 MHz, $CDCl_3$): 0.86 (t, 9H, –CH_3), 1.26–1.32 (m, 60H, –CH_2–), 1.47–1.52 (m, 6H, –CH_2–), 1.73–1.87 (m, 6H, –CH_2–), 4.0–4.09 (m, 6H, –OCH_2–), 7.32 (dd, 2H, aromatic H), 7.40 (s, 2H, aromatic H), 8.19 (dd, 2H, aromatic H).

6.2.4. The polycatenar materials $n\mathbf{PC_mF^{a,b}}$. All the materials $n\mathbf{PC}_m\mathbf{F^{a,b}}$ were synthesized by the same procedure. As a representative method, the synthesis of $\mathbf{14PC_5F^a}$ is described and the structural data of all the materials summarized. To a solution of 0.65 g (0.074 mmol) of the organic acid $\mathbf{8_{14}}$ and 0.6 g (0.074 mmol) of the phenol segment $\mathbf{5_5F^a}$ in 10 ml CH_2Cl_2, a solution of 0.153 g (0.074 mmol) of DCC and 9 mg (0.007 mmol) of DMAP in 5 ml CH_2Cl_2 was added and the mixture stirred overnight. The solvent was evaporated and the residue purified by column chromatography (ethyl acetate/chloroform/hexane=1/1/6) to yield 0.44 g (36%) of $\mathbf{14PC_5F^a}$.

$\mathbf{4PC_5F^a}$: *m/z* 1248 (M^+). Elemental analysis (%): found (calc. for $C_{54}H_{53}O_{14}F_{17}$) C 52.0 (51.93), H 4.5 (4.27), F 25.1 (25.86). ^{1}H NMR (δ_H/ppm, 500 MHz, $CDCl_3$): 0.997 (t, 9H, –CH_3), 1.50–1.58 (m, 2H+6H, –CH_2–), 1.74–1.89 (m, 4H+6H, –CH_2–), 2.42–2.47 (m, 2H, –CH_2COO–), 4.04–4.10 (m, 6H+2H, –CH_2O–),

4.59–4.72 (m, 2H, –$COOCH_2F^a$), 6.97 (d, 2H, Ar–H^g), 7.28 (s, 4H, Ar–H^{e+d}), 7.36 (d, 2H, Ar–H^b), 7.43 (s, 2H, Ar–H^a), 8.15 (d, 2H, Ar–H^c), 8.29 (d, 2H, Ar–H^f). **6PC$_5$F^a**: *m*/*z* 1332 (M^+). Elemental analysis (%): found (calc. for $C_{60}H_{65}O_{14}F_{17}$) C 54.4 (54.06), H 5.1 (4.91), F 24.5 (24.22). ^{1}H NMR (δ_H/ppm, 500 MHz, $CDCl_3$); 0.91 (t, 9H, –CH_3), 1.33–1.38 (m, 12H, –CH_2–), 1.47–1.59 (m, 6H+2H, –CH_2–), 1.71–1.89 (m, 4H+6H, –CH_2–), 2.43–2.47 (m, 2H, –CH_2COO–), 4.04–4.09 (m, 6H+2H, –CH_2O–), 4.63–4.69 (m, 2H, –$COOCH_2F^a$), 6.97 (d, 2H, Ar–H^g), 7.28 (s, 4H, Ar–H^{e+d}), 7.36 (dd, 2H, Ar–H^b), 7.42 (s, 2H, Ar–H^a), 8.15 (dd, 2H, Ar–H^c), 8.29 (dd, 2H, Ar–H^f). **8PC$_5$F^a:***m*/*z* 1416 (M^+). Elemental analysis (%): found (calc. for $C_{66}H_{77}O_{14}F_{17}$) C 56.0 (55.93), H 5.5 (5.47), F 22.3 (22.79). ^{1}H NMR (δ_H/ppm, 500 MHz, $CDCl_3$); 0.89 (t, 9H, –CH_3), 1.29–1.46 (m, 24H, –CH_2–), 1.46–1.59 (m, 6H+2H, –CH_2–), 1.73–1.89 (m, 4H+6H, –CH_2–), 2.43–2.47 (m, 2H, –CH_2COO–), 4.04–4.09 (m, 6H+2H, –CH_2O–), 4.63–4.69 (m, 2H, $COOCH_2F^a$), 6.97 (d, 2H, Ar–H^g), 7.28 (s, 4H, Ar–H^{e+d}), 7.36 (d, 2H, Ar–H^b), 7.42 (s, 2H, Ar–H^a), 8.15 (d, 2H, Ar–H^c), 8.29 (d, 2H, Ar–H^f). **10PC$_5$F^a:***m*/*z* 1500 (M^+). Elemental analysis (%): found (calc. for $C_{72}H_{89}O_{14}F_{17}$) C 57.6 (57.60), H 6.0 (5.97), F 21.9 (21.51). ^{1}H NMR (δ_H/ppm, 500 MHz, $CDCl_3$); 0.885 (t, 9H, –CH_3), 1.28–1.46 (m, 36H, –CH_2–), 1.46–1.59 (m, 6H+2H, –CH_2–), 1.73–1.88 (m, 4H+6H, –CH_2–), 2.43–2.47 (m, 2H, –CH_2COO–), 4.04–4.09 (m, 6H+2H, –CH_2O–), 4.63–4.69 (m, 2H, –$COOCH_2F^a$), 6.97 (d, 2H, Ar–H^g), 7.28 (s, 4H, Ar–H^{e+d}), 7.36 (d, 2H, Ar–H^b), 7.42 (s, 2H, Ar–H^a), 8.15 (d, 2H, Ar–H^c), 8.29 (d, 2H, Ar–H^f). **12PC$_5$F^a**: *m*/*z* 1584 (M^+). Elemental analysis (%): found (calc. for $C_{78}H_{101}O_{14}F_{17}$) C 59.1 (59.08), H 6.4 (6.41), F 21.5 (20.37). ^{1}H NMR (δ_H/ppm, 500 MHz, $CDCl_3$); 0.88 (t, 9H, –CH_3); 1.26–1.46 (m, 48H, –CH_2–), 1.45–1.59 (m, 6H+2H, –CH_2–), 1.71–1.88 (m, 6H+4H, –CH_2–), 2.43–2.47 (m, 2H, –CH_2COO–), 4.04–4.09 (m, 6H+2H, –CH_2O–), 4.62–4.69 (m, 2H, –$COOCH_2F^a$), 6.97 (d, 2H, Ar–H^g), 7.28 (s, 4H, Ar–H^{e+d}), 7.36 (d, 2H, Ar–H^b), 7.42 (s, 2H, Ar–H^a), 8.15 (d, 2H, Ar–H^c), 8.29 (d, 2H, Ar–H^f). **14PC$_5$F^a**: *m*/*z* 1668 (M^+). Elemental analysis (%): found (calc. for $C_{84}H_{113}O_{14}F_{17}$) C 61.0 (60.42), H 6.6 (6.82), F 19.1 (19.43). ^{1}H NMR (δ_H/ppm, 500 MHz, $CDCl_3$): 0.88 (t, 9H, –CH_3–), 1.26–1.37 (m, 60H, –CH_2–), 1.46–1.59 (m, 6H+2H, –CH_2–), 1.71–1.79 (m, 4H, –CH_2–), 1.81–1.89 (m, 6H, –CH_2–), 2.45 (t, 2H, –CH_2CO_2–), 4.04–4.09 (m, 6H+2H, –OCH_2–), 4.66 (q, 2H, –$COOCH_2F^a$), 6.97 (d, 2H, Ar–H^g), 7.28 (s, 4H, Ar–H^{e+d}), 7.36 (d, 2H, Ar–H^b), 7.42 (s, 2H, Ar–H^a), 8.15 (d, 2H, Ar–H^c), 8.29 (d, 2H, Ar–H^f). **16PC$_5$F^a**: *m*/*z* 1752 (M^+). Elemental analysis (%): found (calc. for $C_{90}H_{125}O_{14}F_{17}$) C 61.6 (61.32), H 7.3 (7.13), F 18.6 (18.42). ^{1}H NMR (δ_H/ppm, 500 MHz, $CDCl_3$); 0.88 (t, 9H, –CH_3–), 1.26–1.45 (m, 72H, –CH_2–), 1.47–1.57 (m, 6H+2H, –CH_2–), 1.72–1.88 (m, 6H+4H, –CH_2–), 2.43–2.48 (m, 2H, –CH_2COO–), 4.04–4.10 (m, 6H+2H, –CH_2O–), 4.6–4.7 (m, 2H, –$COOCH_2F^a$), 6.98 (d, 2H, Ar–H^g), 7.28 (s, 4H, Ar–H^e+H^d), 7.36 (d, 2H, Ar–H^b), 7.42 (s, 2H, Ar–H^a), 8.15 (d, 2H, Ar–H^c), 8.29 (dd, 2H, Ar–H^f). **14PC$_5$F^b**: *m*/*z* 1600 (M^+). Elemental analysis (%): found (calc. for $C_{84}H_{115}O_{12}F_{15}$) C 63.1 (63.0), H 7.4 (7.2), F 17.0 (17.8). ^{1}H NMR (δ_H/ppm, 500 MHz, $CDCl_3$): 0.88 (t, 9H, –CH_3–), 1.26–1.37 (m, 60H, –CH_2–), 1.45–1.59 (m, 6H+2H, –CH_2–), 1.71–1.80 (m, 4H, –CH_2–), 1.82–1.88 (m, 6H, –CH_2–), 2.42 (t, 2H, –CH_2CO_2–), 2.46–2.54 (m, 2H, F^b–CH_2–$\underline{CH_2}$–OOC–), 4.04–4.10 (m, 6H+2H, –OCH_2–), 4.40 (t, 2H, F^b–$\underline{CH_2}$–CH_2–OOC–), 6.97 (dd, 2H, Ar–H^g), 7.26 (bs, 2H, Ar–H^d), 7.28 (bs, 2H, Ar–H^e), 7.36 (dd, 2H, Ar–H^b), 7.42 (s, 2H, Ar–H^a), 8.15 (dd, 2H, Ar–H^c), 8.29 (dd, 2H, Ar–H^f). **14PC$_4$F^a**: *m*/*z* 1654 (M^+). Elemental analysis (%): found (calc. for $C_{83}H_{111}O_{14}F_{17}$) C 60.2 (60.2), H 6.7 (6.8), F 19.8 (19.5). ^{1}H NMR (δ_H/ppm, 500 MHz, $CDCl_3$): 0.88 (t, 9H, –CH_3–), 1.26–1.37 (m, 60H, –CH_2–), 1.45–1.55 (m, 6H, –CH_2–), 1.75–1.88 (m, 4H+6H, –CH_2–), 2.51 (t, 2H, –CH_2CO_2–), 4.04–4.10 (m, 6H+2H, –OCH_2–), 4.66 (q, 2H, –$COOCH_2F^a$), 6.97 (dd, 2H, Ar–H^g), 7.29 (bs, 4H, Ar–H^{e+d}), 7.36 (dd, 2H, Ar–H^b), 7.42 (s, 2H, Ar–H^a), 8.15 (dd, 2H, Ar–H^c), 8.29 (dd, 2H, Ar–H^f).

References

[1] S. Chandrasekhar, B.K. Sadashiva, K.A. Suresh. *Pramana*, **9**, 471 (1977).

[2] J. Billard, J.C. Dubois, H.T. Nguyen, A. Zann. *Nouv. J. Chim.*, **2**, 535 (1978).

[3] C. Tschierske. *Annu. Rep. Prog. Chem., Sect. C*, **97**, 191 and references therein (2001).

[4] C. Tschierske. *J. mater. Chem.*, **11**, 2647 and references therein (2001).

[5] J.W. Goodby, G.H. Mehl, I.M. Saez, R.P. Tuffin, G. Mackenzie, R. Auzély-Velty, T. Benvegnu, D. Plusquellec. *Chem. Commun.*, 2057 and references therein (1998).

[6] J. Malthête, A.M. Levelut, H.T. Nguyen. *J. Phys. (Paris) Lett.*, **46**, L875 (1985).

[7] J. Malthête, H.T. Nguyen, C. Destrade. *Liq. Cryst.*, **13**, 171 (1993).

[8] D. Fazio, C. Mongin, B. Donnio, Y. Galerne, D. Guillon, D.W. Bruce. *J. mater. Chem.*, **11**, 2852 (2001).

[9] K.E. Rowe, D.W. Bruce. *J. mater. Chem.*, **8**, 331 (1998).

[10] M.-A. Guillevic, T. Gelbrich, M.B. Hursthouse, D.W. Bruce. *Mol. Cryst. liq. Cryst.*, **362**, 147 (2001).

[11] A.M. Levelut, J. Malthêthe, C. Destrade, N.T. Nguyen. *Liq. Cryst.*, **2**, 877 (1987).

[12] H.T. Nguyen, C. Destrade, J. Malthête. In *Handbook of Liquid Crystals*, Vol. 2B, D. Demus, J.W. Goodby, G.W. Gray, H.W. Spiess, V. Vill (Eds), p. 865, Wiley-VCH, Weinheim, and references therein (1998).

[13] K. Kubo, T. Sutoh, A. Mori, S. Ujiie. *Bull. chem. Soc. Jpn.*, **75**, 1353 (2002).

[14] B. Heinrich, K. Praefcke, D. Guillon. *J. mater. Chem.*, **7**, 1363 (1997).
[15] B. Donnio, B. Heinrich, T.-G. Krzywicki, H. Delacroix, D. Guillon, D.W. Bruce. *Chem. Mater.*, **9**, 2951 (1997).
[16] L. Douce, T.H. Diep, R. Ziessel, A. Skoulios, M. Césario. *J. mater. Chem.*, **13**, 1533 (2003).
[17] C.K. Lai, C.-H. Tsai, Y.-S. Pang. *J. mater. Chem.*, **8**, 1355 (1998).
[18] N. Usol'tseva, P. Espinet, J. Buey, J.L. Serrano. *J. mater. Chem.*, **7**, 215 (1997).
[19] H. Horie, A. Takagi, H. Hasebe, T. Ogawa, K. Ohta. *J. mater. Chem.*, **11**, 1063 (2001).
[20] J. Höpken, C. Pugh, W. Richtering, M. Möller. *Makromol. Chem.*, **189**, 911 (1988).
[21] F. Tournilhac, L.M. Blinov, J. Simon, S.Y. Yablonsky. *Nature*, **359**, 621 (1992).
[22] F.G. Tournilhac, L. Bosio, J. Simon, L.M. Blinov, S.Y. Yablonsky. *Liq. Cryst.*, **14**, 405 (1993).
[23] A.C. Small, D.A. Hunt, C. Pugh. *Liq. Cryst.*, **26**, 849 (1999).
[24] F. Guittard, E.T. de Givenchy, S. Geribaldi, A. Cambon. *J. fluorine Chem.*, **100**, 85 (1999).
[25] S. Diele, D. Lose, H. Kruth, G. Pelzl, F. Guittard, A. Cambon. *Liq. Cryst.*, **21**, 603 (1996).
[26] D. Lose, S. Diele, G. Pelzl, E. Dietzmann, W. Weissflog. *Liq. Cryst.*, **24**, 707 (1998).
[27] T.A. Lobko, B.I. Ostrovskii, A.I. Pavluchenko, S.N. Sulianov. *Liq. Cryst.*, **15**, 361 (1993).
[28] H.T. Nguyen, G. Sigaud, M.F. Achard, F. Hardouin, R.J. Twieg, K. Betterton. *Liq. Cryst.*, **10**, 389 (1991).
[29] T. Doi, Y. Sakurai, A. Tamatani, S. Takenaka, S. Kusabayashi, Y. Nishihata, Teraushi . *J. mater. Chem.*, **1**, 169 (1991).
[30] E. Nishikawa, J. Yamamoto, H. Yokoyama. *Chem. Commun.*, 420 (2003).
[31] E. Nishikawa, J. Yamamoto, H. Yokoyama. *J. mater. Chem.*, **13**, 1887 (2003).
[32] E. Nishikawa, J. Yamamoto, H. Yokoyama. *Liq. Cryst.*, **30**, 785 (2003).
[33] A. Kotzev, A. Laschewsky, R.H. Rakotoaly. *Macromol. Chem. Phys.*, **202**, 3257 (2001).